Pharm Res (2015) 32:1714–1726
DOI 10.1007/s11095-014-1569-y

RESEARCH PAPER

Bridging Laboratory and Large Scale Production: Preparation and *In Vitro*-Evaluation of Photosensitizer-Loaded Nanocarrier Devices for Targeted Drug Delivery

Susanne Beyer • Li Xie • Susanna Gräfe • Vitali Vogel • Kerstin Dietrich • Arno Wiehe • Volker Albrecht • Werner Mäntele • Matthias G. Wacker

Received: 25 August 2014 / Accepted: 4 November 2014 / Published online: 19 November 2014

ABSTRACT

Purpose Industrial production of nanosized drug delivery devices is still an obstacle to the commercialization of nanomedicines. This study encompasses the development of nanoparticles for peroral application in photodynamic therapy, optimization according to the selected product specifications, and the translation into a continuous flow process.

Methods Polymeric nanoparticles were prepared by nanoprecipitation of Eudragit® RS 100 in presence and in absence of glycofurol. The photosensitizer temoporfin has been encapsulated into these carrier devices. Process parameters were optimized by means of a Design of Experiments approach and nanoparticles with optimal characteristics were manufactured by using microreactor technology. The efficacy was determined by means of cell culture models in A-253 cells.

Results Physicochemical properties of nanoparticles achieved by nanoprecipitation from ethanolic solutions were superior to those obtained from a method based upon glycofurol. Nanoencapsulation of temoporfin into the matrix significantly reduced toxicity of this compound, while the efficacy was maintained. The release profiles assured a sustained release at the site of action. Finally, the transfer to continuous flow technology was achieved.

Conclusion By adjusting all process parameters, a potent formulation for application in the GI tract was obtained. The essential steps of process development and scale-up were part of this formulation development.

KEYWORDS Design of Experiments · Drug targeting · Eudragit® RS 100 · Nanoparticles · Photodynamic therapy

ABBREVIATIONS

API	Active pharmaceutical ingredient
AUC	Analytical ultracentrifugation
DLS	Dynamic light scattering
DMEM	Dulbecco's Modified Eagle Medium
DoE	Design of Experiments
FCS	Fetal calf serum
GI	Gastrointestinal
GMP	Good manufacturing practice
mTHPC	meso-tetrakis(3-hydroxyphenyl)chlorin
MWCO	Molecular weight cut-off
PAT	Process analytical technology
PDI	Polydispersity index
PDT	Photodynamic therapy
PEG	Polyethylene glycol
PMS	N-methyl dibenzopyrazine methyl sulphate
S.D.	Standard deviation
SEC	Size exclusion chromatography
SEM	Scanning electron microscopy
SNS ratio	Solvent-to-non solvent ratio
TEM	Transmission electron microscopy
XTT	Sodium 3'-[(phenylaminocarbonyl)-3, 4-tetrazolium]-bis(4-methoxy-6-nitro) benzene sulfonic acid

S. Beyer • K. Dietrich
Institute of Pharmaceutical Technology, Goethe University
Max-von-Laue-Str. 9, 60438 Frankfurt (Main), Germany

L. Xie • V. Vogel • W. Mäntele
Institute of Biophysics Goethe University Max-von-Laue-Str. 1
60438 Frankfurt (Main), Germany

S. Gräfe • A. Wiehe • V. Albrecht
biolitec research GmbH, Otto-Schott-Str. 15, 07745 Jena, Germany

M. G. Wacker (✉)
Department of Pharmaceutical Technology Fraunhofer-Institute for Molecular Biology and Applied Ecology IME, Project group for Translational Medicine & Pharmacology TMP Max-von-Laue-Str. 9
60438 Frankfurt (Main), Germany
e-mail: matthias.wacker@ime.fraunhofer.de

INTRODUCTION

Over the past decades, extensive research activities have focused on the development of colloidal drug delivery devices for targeting an active pharmaceutical ingredient (API) to the specific site of action, e.g. the vascular system [1] or the gastrointestinal (GI) tract [2, 3]. Unfortunately, only little attention has been paid to these prototypes by the pharmaceutical industry and only a limited number of drug formulations have been approved so far. Nanoformulations of high complexity but with a considerable *in vitro*- and *in vivo*-performance are described in the literature. In many cases the transfer to industrial manufacture cannot be achieved with current technologies [4].

One related reason is the absence of appropriate preparation methods and a rational formulation design that would allow the production of these nanocarriers at a large scale while the pharmaceutical quality is maintained [1]. Amongst other technologies, nanoprecipitation has been utilized for the preparation of polymeric nanoparticles at the laboratory scale [5, 6]. In principle, encapsulation of the API is achieved by desolvation of polymer and compound with an aqueous solution of an amphiphilic stabilizer. Process conditions are adjusted with regard to the reaction vial, stirring speed, the concentration of all reactants, and the pumping rate that controls the amount of added non-solvent [6].

Recently, microfluidic platform technologies have been applied to the continuous flow production of nanoparticles. However, major shortcomings of these approaches have been a clogging of the nozzle or the reaction chamber due to narrow capillaries and the limited output as a result of restrictions in the amount of substance passing through the capillaries [7, 8]. Moreover, particles yielded by microreactor-assisted nanoprecipiation are often characterized by a broad size distribution [9].

The current approach contrasts two nanocarrier devices for targeted drug delivery by using a multitude of analytical technologies. An optimized experimental design supported the process development and allowed the production of these nanocarriers within a defined specification range. Moreover, the transfer of this formulation to a medium scale production was achieved by microreactor-assisted nanoprecipitation [10]. This technique allows the preparation of high nanoparticle amounts [8, 9]. Precipitation of the polymer in the microfluidic platform is initiated by controlled mixing of the polymer solution with a non-solvent at a defined angle, ratio, and speed [9–11]. By means of this process, photosensitizer-loaded nanocarrier devices for peroral administration have been generated.

Photosensitizers are light-sensitive molecules that are activated by illumination with infrared or visible light. By transition into the excited state in the presence of oxygen, reactive singlet oxygen is generated which induces cell death in malignant tissues. It elicits photodestruction of the vasculature that is accompanied by local hypoxia and indirect cell death [12]. The compound meso-tetrakis(3-hydroxyphenyl)chlorin (mTHPC), also known as temoporfin, is characterized by poor aqueous solubility and a number of side effects that occur after systemic distribution of the API into tissues that are exposed to light sources [13], e.g. the eyes or the skin [14]. Size-controlled local accumulation in inflamed tissues of the GI tract and low systemic availability of the photosensitizer were the most important criteria for the presented formulation design.

Photosensitizer-loaded nanoparticles have been manufactured from polymethacrylic acid in combination with ethanol or the water-miscible polymer glycofurol. While ethanol evaporates more rapidly from the achieved suspensions, glycofurol is embedded into the polymer matrix. Consequently, the formulation composition plays a pivotal role with regards to desolvation velocity, precipitation efficiency and therefore the achieved particle properties.

In summary, the major objectives have been the selection of an optimized formulation design for the preparation of photosensitizer-loaded nanoparticles and the translation of particle manufacture into a medium scale process that assures a high quality with regards to the most relevant product specifications.

MATERIALS AND METHODS

Chemicals and Reagents

Tetrahydrofurfuryl alcohol polyethylene glycol ether, also known as glycofurol (lot S6224192 145) was purchased from Merck Schuchardt OHG (Hohenbrunn, Germany). Polysorbate 20 (lot 9005-65-6) was purchased from Fluka Chemika (Buchs, Germany). Eudragit® RS 100 (lot E100108020) was kindly provided by Evonik Röhm GmbH (Darmstadt, Germany). mTHPC, also known as temoporfin (lot 081112) was kindly provided by biolitec research GmbH (Jena, Germany). Trifluoroacetic acid (purity >99.8%, lot ZA 3765762) and lithium chloride (lot B0726979 202) were purchased from Merck KGaA (Darmstadt, Germany). Methyl-β-cyclodextrin (lot STBC7393V) was purchased from Sigma-Aldrich Chemie GmbH (Munich, Germany). Spectra/Por® 6 dialysis tubing, molecular weight cut-off (MWCO) 50,000 Da, regenerated cellulose, diameter 18 mm (lot 3264673) was purchased from Serva Electrophoresis GmbH (Heidelberg, Germany). Dulbecco's Modified Eagle Medium (DMEM), heat-inactivated fetal calf serum (FCS) and penicillin-streptomycin solution were purchased from PAA Laboratories GmbH (Egelsbach, Germany). A-253 cells were purchased from ATCC Inc. (Manassas, USA). Sodium 3'-[(phenylaminocarbonyl)-3,4-tetrazolium]-bis(4-methoxy-6-nitro)benzene sulfonic acid (XTT) and N-methyl

dibenzopyrazine methyl sulphate (PMS) were purchased from AppliChem GmbH (Darmstadt, Germany).

Preparation and Characterization of Eudragit® RS 100 Nanoparticles

Preparation of Eudragit® RS 100 Nanoparticles at the Small Scale

Nanoprecipitation was performed in small scale according to a refined version of the experimental setup described earlier by Bodmeier *et al.* and Viehof *et al.* [15, 16]. The matrix material Eudragit® RS 100 was dissolved either in ethanol 96% [v/v] or in glycofurol. The concentrations of the polymer solutions were adjusted to values ranging from 10 to 25% [w/v], respectively.

While continuously stirred at 550 rpm, an aqueous solution of polysorbate 20 at a concentration of 0.01% [w/v] was added dropwise by utilizing a peristaltic pump (ISM837B; Ismatec, IDEX Health & Science GmbH, Wertheim, Germany) and induced the precipitation of the polymer. The obtained suspensions were stirred overnight at room temperature [17].

Design of Experiments (DoE) Based on the Small Scale Approach

Design-Expert® software version 8 (Stat-Ease Inc., Minneapolis, USA) was used to evaluate the impact of multiple process parameters on particle characteristics. Therefore, the D-optimal design was applied.

The impact of precipitation speed was analyzed by adjusting the flow rate to values ranging from 1 to 12 mL/min (see Table 1). For these experiments, an absolute amount of 1 mL polymer solution was precipitated with 4 mL of the polysorbate 20 solution. Eventually, effects on particle diameter, polydispersity index (PDI), and the zeta potential were determined by dynamic light scattering (DLS) in combination with microelectrophoresis.tgroup

Polynomial analysis and ANOVA were performed for the three response parameters. The quadratic model was utilized for particle size, whereas for the PDI the linear model and for zeta potential the 2FI model was used for calculation.

Determination of the Particle Properties by DLS

The suspensions achieved by nanoprecipitation were diluted 50-fold with purified water and analyzed by DLS utilizing a Zetasizer Nano ZS (Malvern Instruments GmbH, Malvern, UK) with a backscatter detector at an angle of 173 °. Additionally, the zeta potential was determined by microelectrophoresis in a Malvern dip cell.

Visualization of Particle Size and Shape by Transmission Electron Microscopy (TEM)

A volume of 20 µL of the nanocarrier suspensions was transferred onto a coated copper grid. The polymer particles were stained with phosphotungstic acid solution at a concentration of 2% [w/v]. Afterwards, the characteristics of Eudragit® RS 100 nanoparticles were examined by TEM. For this purpose a transmission electron microscope CM 12 (Philips, Amsterdam, Netherlands) equipped with a Gatan module 782 (ES 500 W) was used.

Visualization of Particle Size and Shape by Scanning Electron Microscopy (SEM)

Nanoparticles were prepared as described above. An aliquot of the particle suspensions (20 µL) was placed on a sample holder and allowed to dry over 24 h. Afterwards, the samples were sputtered with gold, using an Agar Sputter Coater (Agar Scientific, Essex, UK). Electron microscopy was performed with a Hitachi S4500 microscope system (Hitachi, Tokyo, Japan) at an accelerating voltage of 15 kV.

Determination of Particle Properties by Analytical Ultracentrifugation (AUC)

Polymer nanoparticles were diluted 50-fold with 15 mM sodium chloride solution to concentrations that correspond to apparent turbidities in the range of 0.3 to 0.8. The AUC experiments were performed by using a Beckman Optima XL-A ultracentrifuge, an An-50Ti rotor, and double-sector charcoal-filled Epon centerpieces with an optical path length of 12 mm. The rotor speed was adjusted to 10,000 or 30,000 rpm for both samples and the rotor temperature was maintained at 20°C. Volumes of 300 and 310 µl were used for sample and reference, respectively. Data of the apparent absorbance (turbidity) versus radius were collected at 320 nm, using a radial step size of 0.03 mm [18, 19]. For the analysis of the particle size distribution, the sedimentation velocity data were modelled as a distribution of non-diffusing particles based on the observations of large sedimentation coefficients and of large

Table I DoE: Variables and levels used in the D-optimal design for nanoprecipitation of Eudragit® RS 100 solution.

Factor	Name	Units	Type	Levels	Level 1	Level 2	Level 3	Level 4
A	polymer concentration	[%; m/v]	Numeric	4	10	15	20	25
B	flow rate	[mL/min]	Numeric	4	1	5	10	12
C	solvent		Categoric	2	Ethanol	Glycofurol		

particle diameters gained from DLS measurements [18, 20]. For calculation of the apparent sedimentation coefficient distribution g*(s), least-squares boundary modelling with the program sedfit by P. Schuck was used (available from: http://www.analyticalultracentrifugation.com) [18, 20].

Determination of Precipitation Efficiency

The particle yield was determined by size exclusion chromatography (SEC) of the polymer Eudragit® RS 100. The HPLC-system (Merck Hitachi LaChrom, Tokyo, Japan) was composed of an L-6220 pump, an L-7350 column oven, an L-7200 autosampler, a differential refractometer detector RI-72 and a D-7000 interface. The quantification method for polymethacrylic acid was adjusted from the one described by Porsch *et al.* [21].

A Biosep SEC S-3000-column (Phenomenex Inc., Aschaffenburg, Germany) was used as stationary phase. Ethanol 96% [v/v] containing 100 mM lithium chloride served as the mobile phase. Detection was accomplished with the help of a refractive index detector. The flow rate was set to 1 mL/min and an injection volume of 40 μL was used.

All samples were purified by centrifugation of 1 mL of the nanoparticle suspension (16,100 rcf, 15 min at room temperature) and redispersion in purified water. The solid pellet obtained from the second centrifugation step was dissolved in the mobile phase and injected into the HPLC system. Linearity of quantification method was assured in a range from 5 to 50 mg/mL.

Encapsulation of the Photosensitizing Agent mTHPC into the Polymeric Matrix

Photosensitizer-loaded particles were generated by addition of 7.5 mg of the photosensitizer to 1 mL of either ethanolic or glycofurolic polymer solutions at a Eudragit® RS 100 concentration of 15% [w/v]. The desolvation was induced by addition of 4 mL of the aqueous medium at a flow rate of 12 mL/min. The stirring speed was kept constant at 550 rpm throughout this process.

Quantification of the Drug Loading Efficiency

For determination of encapsulation efficiency, a HPLC method described by Dragicevic-Curic *et al.* [22] was used. mTHPC was quantified from the supernatant after centrifugation of the suspension through centrifugal filters (Amicon® Ultra; EMD Millipore Corporation, Billerica, USA) consisting of a regenerated cellulose membrane with a MWCO of 100 kDa. The centrifugate was analyzed for the amount of API.

Filter adsorption of Eudragit® RS 100 and mTHPC was analyzed by centrifugation of organic solutions through the described filter membrane and quantification of these substances from the centrifugate. For quantification, the solutions were diluted and analyzed for the amount of API. A reversed phase column (Gemini NX-C 18; Phenomenex Inc., Aschaffenburg, Germany) as stationary phase, combined with a mobile phase consisting of 47.5% [w/w] trifluoroacetic acid (as an aqueous solution at a concentration of 0.1% [v/v]) and 52.5% [w/w] acetonitrile, were used for the analysis. Flow was set to 1 mL/min, 420 nm was selected as detection wavelength. The HPLC-system (Merck Hitachi, Tokyo, Japan) consisted of an LC-Organizer, a D-6000A interface, a L-4500 diode array detector, an AS-2000A autosampler and a L-6220 intelligent pump.

Purification Procedure

A purification procedure was undertaken to remove residues of the stabilizer and unprecipitated polymer. Therefore, 1 mL nanoparticle suspension was centrifuged at 16,100 rcf for 15 min. The supernatant was decanted and the pellet subsequently resuspended in 1 mL of purified water. The procedure was repeated twice. Drug load was determined from those suspensions after purification using the HPLC method described in Quantification of the Drug Loading Efficiency.

Scale-up Utilizing Microreactor-assisted Nanoprecipitation

For medium scale production of nanoparticles in a continuous flow process, the modular microreactor technology was used. In principle, two streams of liquids are intensively mixed in the reaction chamber at a defined angle and speed before they are subsequently removed by an inert gas stream (Ehrfeld Microtechnic product information 2012).

The system was composed of an A5 base plate, a microjet mixer, three inlet modules (no. 704-1), an outlet module (no. 704–3), and clamping modules (no. 821–3). Two HPLC-pumps L-6200 (Merck Hitachi, Tokyo, Japan) controlled the pumping rate of these liquids (polymer and stabilizer solution; see Fig. 1). For the polymer solution, concentrations of 15, 20, and 25% [m/v] Eudragit® RS 100 dissolved in ethanol 96% [v/v] were tested. The stabilizer solution was prepared analogously to the experiments performed at the small scale (0.01% [m/v] of polysorbate 20 in aqueous solution). The solvent-to-non solvent ratio (SNS ratio) that is defined by the flow rates of both solutions was primarily set to 1 to 4 (imitating the laboratory scale process) and adjusted to a final SNS ratio of 1 to 3 in further experiments.

Therefore, the flow rate of the polymer solution was set to 0.1 mL/min either combined with a flow rate of 0.3 mL/min (SNS ratio 1 : 3) or 0.4 mL/min (SNS ratio 1 : 4) for the stabilizer solution. This resulted in an absolute flow rate of 0.4 mL/min or 0.5 mL/min, respectively. Alternatively, absolute flow rates of 1.5 mL/min or 2 mL/min were used while

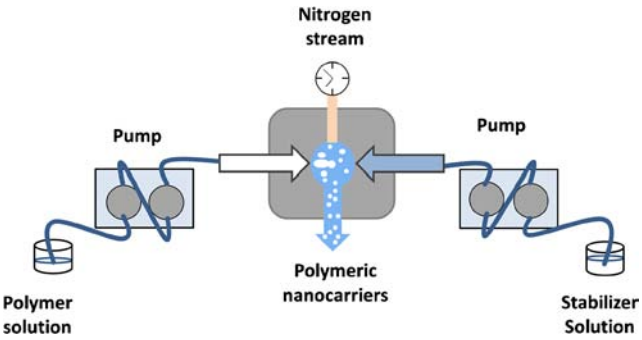

Fig. 1 Schematic illustration of the microfluidic reaction system used for nanoprecipitation in a continuous flow process.

maintaining the described SNS ratios. For all experiments the inlet pressure of nitrogen was set to 500 mbar.

Finally, the process was applied to the preparation of temoporfin-loaded Eudragit® RS 100 nanoparticles. Therefore, a SNS ratio of 1 to 3 was selected. The absolute flow rates were set either to 0.4 mL/min or to 2 mL/min, respectively. A concentration of 15% [w/v] for the polymer Eudragit® RS 100 combined with 7.5 mg/mL of mTHPC, both dissolved in ethanol 96% [v/v] were utilized. All other process parameters were adjusted as described earlier in this section.

In Vitro-characterization

Drug Release from the Nanoparticulate Systems

The dissolution properties of temoporfin-loaded Eudragit® RS 100 nanoparticles prepared from ethanolic solutions were determined before and after the purification process (see Purification Procedure) and compared to the release profile of the pure API.

A dialysis cell system was specifically designed to assess the *in vitro*-release kinetics of nanospheres. The system was composed of two chambers with a volume of 6 mL for the donor compartment and 12.7 mL for the acceptor compartment, respectively. These chambers were separated by a dialysis membrane with a MWCO of 50,000 Da and a surface area of 13.44 cm^2. A flow cuvette was connected to the acceptor compartment to allow an in-line fluorescence measurement (see Fig. 2).

Phosphate buffer (pH 6.8) was used as medium for these release experiments. Methyl-β-cyclodextrin at a concentration of 1 mg/mL was added to maintain sink conditions. Throughout the process, the donor phase was stirred with a speed of 25 rpm and the release medium in the acceptor phase was pumped at a flow rate of 4.5 mL/min through the cuvette.

For in-line fluorescence measurement an OceanOptics microspectrometer (USB4000 Miniature Fiber Optic Spectrometer; Ocean Optics GmbH, Ostfildern, Germany)

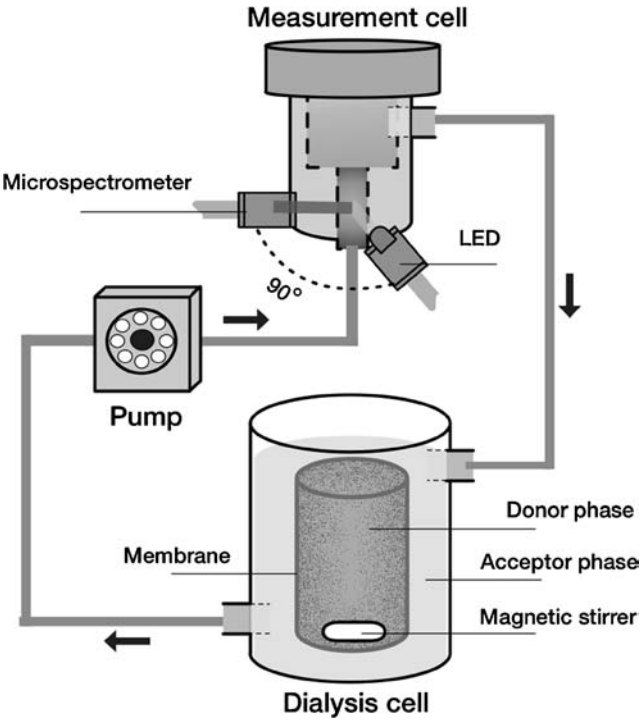

Fig. 2 Setup of the dialysis cell for release experiments of polymeric nanoparticles. In-line measurement was assured by connection to a microspectrometer.

equipped with optical fibers was used. A light-emitting diode with a wavelength of 405 nm (20 mA, 3.5 V) was selected as the excitation light source. Fluorescence intensity was monitored continuously by using the Ocean Optics SpectraSuite® software (Ocean Optics GmbH, Ostfildern, Germany).

All experiments were undertaken in triplicate. The slope within the first 450 min was calculated and one-sample t-test was performed.

Evaluation of Dark Toxicity and Phototoxicity In Vitro in A-253 Cells

A human epidermoid A-253 carcinoma cell line from the submaxillary salivary gland was grown in DMEM supplemented with 10% heat-inactivated FCS, 1% penicillin (10,000 IU) and streptomycin (10,000 μg/mL). The cells were kept at 37°C as monolayer culture in a humidified incubator containing 5% CO_2. A photosensitizer stock solution of mTHPC (2 mM) was assembled in DMSO and kept in the dark at 4°C. Further dilution was performed in DMEM without phenol red supplementation, but with an addition of 10% FCS, to adjust the final photosensitizer concentrations to 0.5 or 2 μM, respectively. Particle systems were diluted similarly to the photosensitizer stock solution.

Three days before treatment, cells were seeded in microplates (2,000 cells/well). Cells were incubated with fresh medium (DMEM without phenol red supplementation) with 0.5 or 2 μM of the photosensitizer solution, or photosensitizer-

loaded particle systems for 24 h before light exposure. Prior to photosensitization, cells were washed, incubated with DMEM without phenol red, but 10% FCS, subsequently irradiated at room temperature with a 652 nm-diode laser (Ceralas® PDT 652 nm; Biolitec AG, Jena, Germany) at a fixed total light dose of 50 J/cm^2, and a fluence rate of 1 W/cm^2. Following the irradiation, cells were incubated for 24 h until the cell viability assay was performed. Cell viability was assessed by the XTT assay. After incubation of the cells with the described formulation or control, the medium in the microplate was replaced by fresh DMEM without phenol red containing 10% FCS, prior to adding 50 µl XTT-reaction solution per well. The microplate was incubated for 2–3 h at 37°C and 5% CO_2. The absorbance of the samples was measured with a spectrophotometer (Tecan Infinite® 200; Tecan Group AG, Männedorf, Switzerland) at a wavelength of 490 nm. By utilizing a wavelength of 630 – 690 nm non-specific absorbance phenomena were effectively excluded. Nanoparticles gained with the excipient ethanol or glycofurol were tested. Furthermore, particles before and after the purification process (see Purification Procedure) were evaluated.

Statistical Analysis

All data are expressed as mean ± standard deviation (S.D.). For the determination of significance, ANOVA was performed for the selected response surfaces in a DoE-setup. Differences were considered to be significant if $p < 0.05$. One-sample t-test with $\alpha = 0.05$ was used in order to evaluate the release experiments.

RESULTS

Preparation and Characterization of Eudragit® RS 100 Nanoparticles

A comprehensive evaluation of particle synthesis was attained by using an optimized experimental design combined with an extensive characterization of the achieved products. During process development the particle size and the size distribution of all particle species were analyzed by using DLS, AUC, TEM, and SEM methods. A rational formulation design was achieved by applying an experimental setup based on DoE for optimization of the drug delivery system.

DoE

The selected mathematical patterns in the DoE assured significance for all selected response parameters. For particle size the quadratic model was utilized ($p = 0.0311$), whereas for the PDI the linear model ($p = 0.0094$), and for the zeta potential 2FI model ($p = 0.0004$) were used for the calculation.

The impact of polymer concentration and flow rate of the non-solvent were determined for both initial formulation designs, with ethanol and glycofurol, in order to optimize the precipitation process for these nanoparticles.

For this experimental setup, precipitation kinetics and therewith particle size were strongly affected by the absolute flow rate, while many other critical parameters, such as the type and dimensions of stirrer and reaction vial, local turbulence, and the overall circulation were kept constant.

Figures 3a and c indicate the properties of particles generated from ethanolic solutions. An increased flow rate resulted in particles of decreased diameters. The desired particle size of less than 200 nm was achieved at a flow rate higher than 5.41 mL/min.

Similar to the experiments conducted with ethanolic Eudragit® RS 100 solutions, the outcome with glycofurol as an excipient was analyzed (see Fig. 3b and d). Since the particle size of 200 nm was achieved already at 1.73 mL/min, this formulation design emerged to be more robust to process changes. The particles were of narrow size distribution as indicated by decreased PDI values (see Fig. 3d). Similar to desolvation from ethanolic solutions, an impact of the polymer amount on the measured particle size could be observed (see Fig. 3a and b).

Visualization of Particle Size and Shape by SEM and TEM

The observations made by electron microscopy revealed that spherical particles were achieved when the polymer was precipitated from ethanolic Eudragit® solutions (see Fig. 4). Particle size was consistent with the results gained by DLS.

An edgy shape was observed for their counterparts generated from glycofurolic solutions (see Fig. 5). Besides these qualitative aspects, the images suggest that a high amount of the generated nanoparticles was significantly smaller than implied by the DLS results (see Fig. 5a).

Determination of Particle Properties by AUC

Since electron microscopy and DLS are of limited value for the quantitative analysis of particle size distribution for multimodal distributed colloids, AUC was utilized to investigate the influence of the formulation design on this parameter. AUC experiments indicated that particles obtained from glycofurolic solutions were substantially smaller than the ones generated from ethanolic solutions (see Fig. 6). The colloids manufactured by using the ethanolic desolvation method were characterized by a broader size distribution which was also indicated by the increased PDI compared to other formulations, e.g. particles consisting of human serum albumin [23].

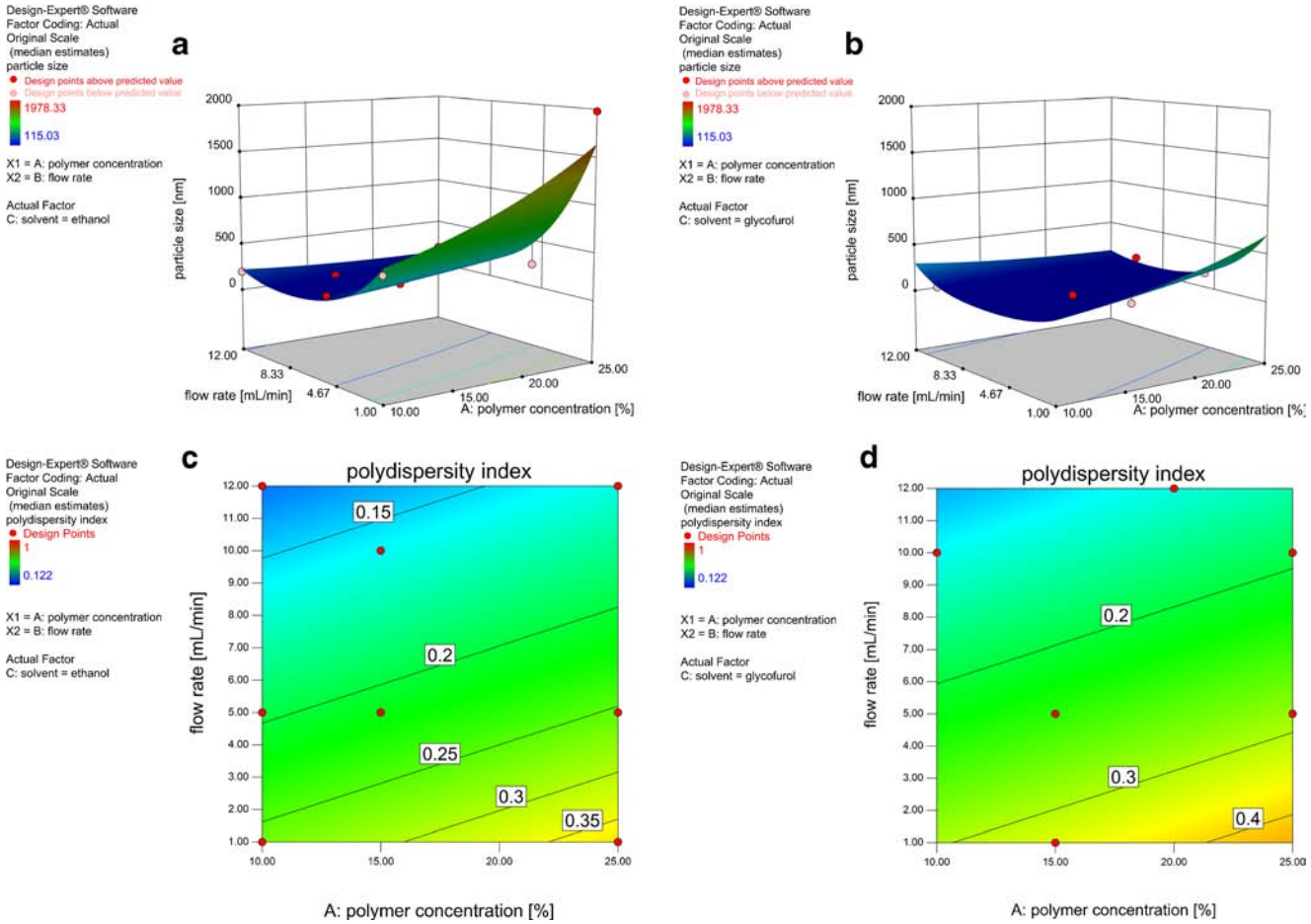

Fig. 3 DoE: Impact of varied process parameters (polymer concentration and flow rate) on particle size and PDI. Figures a and c illustrate the experiments performed with ethanol, b and d with glycofurol. D-optimal design with quadratic fitting was applied.

From the DLS measurements, nanoprecipitation in presence of glycofurol emerged to be superior to ethanolic desolvation. Under these conditions the slow pumping rates still resulted in nanoparticles with a rather narrow size distribution (see Fig. 3).

However, for the glycofurolic system, size fractions seen in the AUC apparently did not cover the rare, but still present particles of larger diameters (see Fig. 5a). Consequently, the size distribution of this formulation design can only be explained by taking into account a combination of all analytical techniques.

Determination of Precipitation Efficiency

The amount of polymer that was converted into nanoparticles was quantified by SEC. Samples that were prepared by nanoprecipitation from 15% [w/v] Eudragit® RS 100 dissolved in either ethanol or glycofurol, with a desolvation speed of 12 mL/min, were contrasted after centrifugation of the dispersion. When ethanol was employed as a solvent, a particle yield of 28.62±0.7% was achieved. For the formulation design that contained glycofurol, the effective precipitation yield was 4.17±0.1%.

Quantification of the Drug Loading Efficiency

For the indirect quantification of the filtrate of particle suspensions, encapsulation efficiencies higher than 72% were determined for both formulation designs. In principle, the drug loading efficiency was higher when precipitation was performed from ethanolic solution (78.65±4.8%). When glycofurol was used, drug loading efficiency was determined to be 72.54±6.5%. Filter absorption was tested and found to be lower than 0.1% for mTHPC. However, the polymer Eudragit® RS 100 absorbed to the filter to an extent of 27% suggesting that (in aqueous suspension) the combination of both components, Eudragit® and API, adheres to the filter membrane. Quantifying the drug load after purification revealed a drug loading efficiency of 3.12±1.4% for the glycofurol-based formulation. When ethanol was used, the drug load increased to a value of 25.79±0.8%.

It is evident that a high amount of API was in the supernatant. Therefore, the interactions of unprecipitated polymer and API will be further evaluated and discussed taking into account the release properties in upcoming sections.

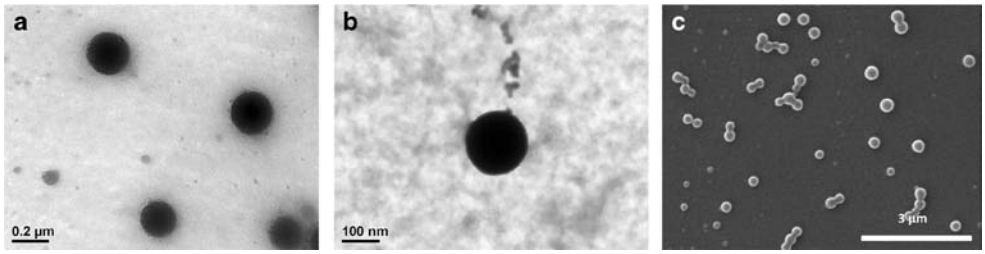

Fig. 4 Images recorded by TEM (**a** and **b**) after staining of Eudragit® RS 100 nanoparticles with phosphotungstic acid, or SEM (**c**) after sputtering with gold. Particles were achieved by precipitation from ethanolic polymer solutions.

Since the experimental setup for particle separation was similar to the quantification of precipitation efficiency, a drug binding of 78.65 ± 4.8% to the polymer with 28.6 ± 0.7% (see Determination of Precipitation Efficiency) of particles in the selected size range is probable for the ethanolic approach. These particles contain 25.79 ± 0.8% of the mTHPC used for the manufacturing process.

Drug Release from the Nanoparticulate Systems

The correlation of released mTHPC over time is illustrated in Fig. 7. A more rapid release was observed for the pure API, while the nanoparticulate systems demonstrated a significantly reduced slope under accelerated conditions in the corresponding release profiles. Differences between purified and non-purified formulations were negligible. Since there were no significant differences observed in the release profiles of the different batches, reproducibility of the manufacturing process was demonstrated.

Evaluation of Dark Toxicity and Phototoxicity In Vitro in A-253 Cells

Since encapsulation of the API into the matrix material changes the microenvironment of the photosensitizer, a reduction in photodynamic activity as a consequence of the formulation design was excluded by assessment of the photo- and dark toxicity *in vitro*.

For the API encapsulated into nanoparticles, the toxicity on A-253 cells after illumination was not decreased, regardless of the utilized solvent (see Fig. 8). By encapsulation into the polymeric matrix a decreased toxicity of the API in the dark control could be achieved. Moreover, the differences between purified and not purified formulations were negligible independently of the utilized solvent.

Scale-up Utilizing Microreactor-assisted Nanoprecipitation

Approaching industrial scale manufacture, microreactor-assisted nanoprecipitation was applied. This elegant technique allows production of nanocarriers in a scalable continuous-flow process. The influence of previously determined parameters on the important product characteristics was investigated and nanoparticles prepared at the small and at medium scale were compared.

Influence of Absolute Flow Rate and Polymer Concentration

The mixing chamber as centerpiece of the microreactor system assured fast and intensive mixing of the two liquids and thereby confirmed a distinct control of precipitation kinetics by adjusting the absolute flow rate and polymer concentration. Since all other parameters were defined by the dimensions of the reactor, variables investigated profoundly at the small scale approach did not differ strongly from those that affected the product in a continuous flow process. In consequence, particle properties were precisely controlled.

For small scale experiments, dimensions of the reaction vial and stirring bar were kept constant, and the SNS ratio was adjusted to 1 to 4. Consequently, flow rates of 0.5 mL/min for the polymer solution and of 2.0 mL/min for the stabilizer solution, combined with a polymer concentration of 15% [w/v], were selected in the microreactor initially.

These particles were significantly smaller than those obtained by laboratory scale preparation (particle size 89.6 ± 1.3

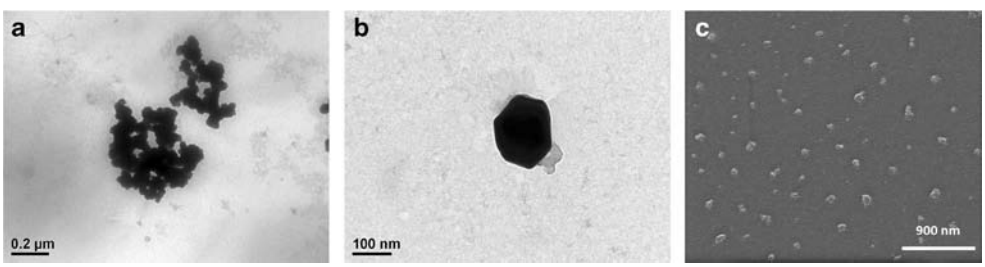

Fig. 5 Images recorded by TEM (**a** and **b**) after staining of Eudragit® RS 100 nanoparticles with phosphotungstic acid, or SEM (c) after sputtering the particles with gold. Particles were achieved by precipitation from glycofurolic polymer solutions.

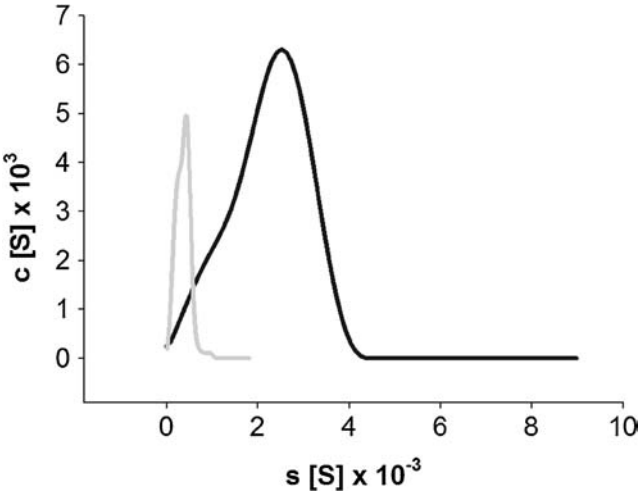

Fig. 6 Sedimentation coefficient distribution of nanoparticles generated by precipitation from glycofurol (grey) or ethanol (black) in lab scale.

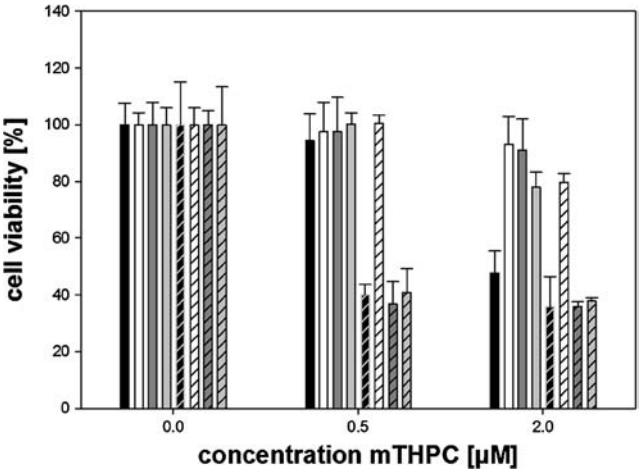

Fig. 8 Viability of A-253 cells after incubation with pure mTHPC (black), Eudragit® nanoparticles containing no mTHPC (white), mTHPC-loaded particles (not purified; dark grey) and mTHPC-loaded particles (purified; light grey). Samples were either tested in the absence of light (no pattern) or after laser illumination (with pattern). All particles systems were prepared from ethanolic solutions. S.D. was used for descriptive error bars.

nm; see Fig. 9). Since the investigated flow rates did not result in nanocarriers completely comparable to the counterparts generated on the stirring plate, the absolute flow rate was adjusted to 0.5 mL/min without changing the SNS ratio. These results confirmed an increase in particle diameter when decreasing absolute flow rates (particle size 137.8±5.0 nm).

In further experiments the SNS ratio was altered. Adjusting this ratio to 1 to 3, absolute flow rates of 2 mL/min and 0.4 mL/min were tested. The resulting particles were characterized by enlarged diameters (see Fig. 9), and furthermore by a narrow size distribution (PDI <0.3; see Fig. 9).

Figure 10 outlines the effect of various polymer concentrations on particle diameter. As seen for the small scale precipitation method, highly concentrated polymer solutions increased the size of the nanocarriers. However, that size distribution was shifted to nanoparticles of larger diameter under the examined circumstances, as it was indicated by rising PDI values.

Hence, the nanoprecipitation process was controlled in the modular system by alteration of the absolute flow rates, the SNS ratio, and the polymer concentration. For encapsulation of the photosensitizer mTHPC, a SNS ratio of 1 to 3 and absolute flow rates of 0.4 mL/min or 2 mL/min were tested in combination with Eudragit® concentrations of 15% [m/v].

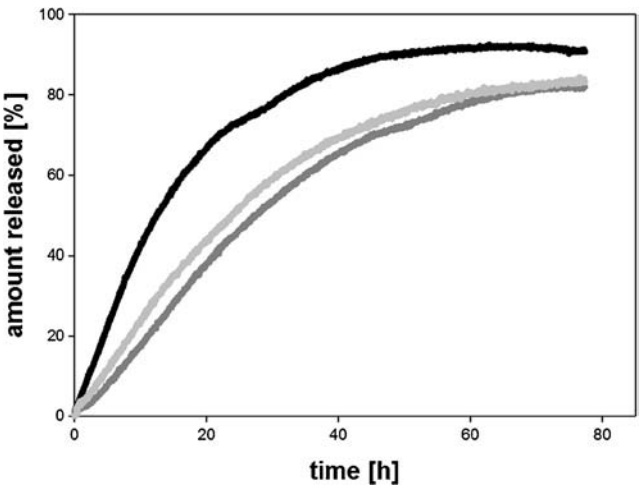

Fig. 7 Release of mTHPC and the corresponding nanoparticles through a membrane with a MWCO of 50 kDA. Pure mTHPC (black), mTHPC-nanoparticles that were purified (dark grey) or not purified (light grey) were tested for 80 h. A total drug amount of 50 μg mTHPC was used in all cases.

Quantification of the Drug Loading Efficiency and Precipitation Efficiency of Temoporfin-loaded Particles Prepared by Microreactor-assisted Nanoprecipitation

Similar to the small scale experiments, the amount of mTHPC encapsulated into nanoparticles was quantified. At lower flow rates, the indirect quantification revealed a drug loading efficiency of 99.97±0.1%. For the higher flow rates, drug load was found to be 99.93±0.1%. Precipitation efficiency was determined to be 15.53±2.0% for the lower flow rates and 33.14±5.2% for the high flow rates, respectively.

These results confirm the preparation of drug-loaded nanocarrier devices comparable to those generated at the laboratory scale.

Visualization of Nanocarriers from Microreactor-assisted Nanoprecipitation by SEM

Observations in the SEM (see Fig. 11) revealed that the continuous flow-method resulted in particles with characteristics similar in shape to those gained from the small scale experiments.

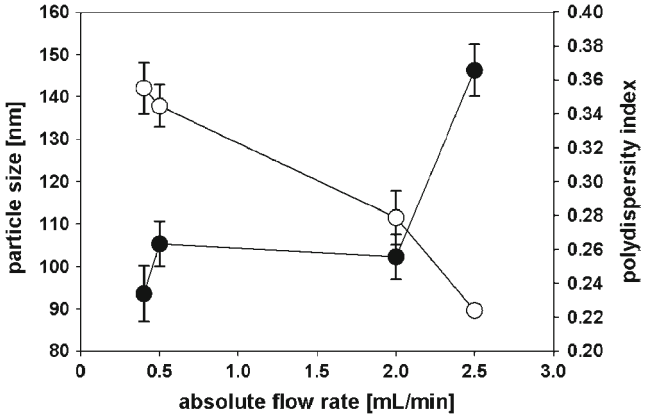

Fig. 9 Impact of absolute flow rate (summation of stabilizer and polymer flow) on particle size (white) and PDI (black) of Eudragit® RS 100 particles generated with microreactor technique. The experiments were conducted in triplicate. S.D. was used for descriptive error bars.

DISCUSSION

Pharmaceutical quality issues are one major obstacle to the production and commercial success of nanocarrier devices [1, 24]. Since the regulatory authorities in Europe and the USA demand a comprehensive physicochemical characterization of nanosized drug delivery systems, these aspects were considered during the optimization of nanoparticle manufacture. This includes parameters relevant to the targeted delivery of nanocarriers in the GI tract such as colloid size, size distribution, particle shape, net charge, particle yield, encapsulation efficiency, and the release behavior [25].

For the selection of these characteristics, the pathophysiological conditions in inflammatory bowel disease and cancer were predominantly important. With regards to inflammatory bowel disease, an elevated mucus production, an increased number of immune related cells, and an enhanced permeability of the GI barrier have been considered [26]. Those conditions are addressed by small particles (size <1 μm) that consist of a mucoadhesive material [3]. Similar claims have been observed for an effective targeting of tumor cells [27]. Abnormalities in the vascular system accompanied by increased permeability enable the transport of particles in the size range of 20 to 200 nm into the affected tissue [27].

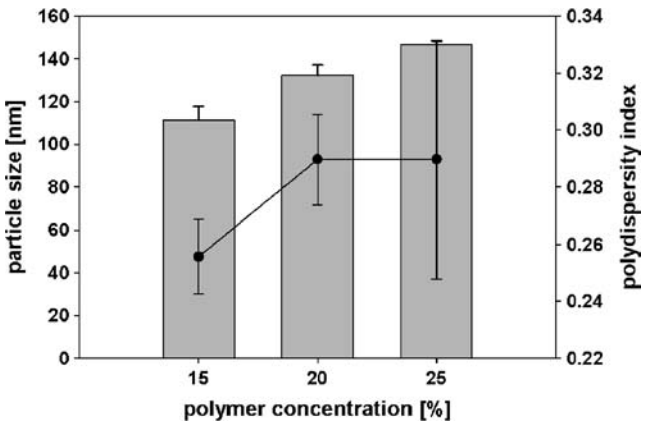

Fig. 10 Impact of the amount of Eudragit® RS 100 in ethanolic solutions on size (grey bars) and size distribution as indicated by PDI (black dots) of the manufactured nanoparticles by microreactor technology. Flow rate of polymer solution was set to 0.5 mL/min; for the stabilizing solution a flow of 1.5 mL/min was used. All experiments were performed in triplicate. S.D. was used for descriptive error bars.

Therefore, process parameters have been adjusted in order to synthesize particles within a defined size range of 100 to 200 nm. A narrow size distribution was of major importance to quantitatively address this specification. For a valid determination of size distribution by DLS, the algorithms that are used for calculation of the PDI have their optimum in a range between 0.08 and 0.7. A PDI below 0.3 is typically used as threshold to assure a monodisperse size distribution [28].

With Eudragit® RS 100, a positively charged sustained release polymer has been chosen for the initial formulation design. By this means, the risk of systemic exposure to the API has been significantly reduced.

Initially, two different formulation designs (formulations with glycofurol or ethanol) have been selected for further experiments. DoE analysis revealed that both methods allowed distinct control of the particle preparation with focus on the desired size range by adjusting the independent variables flow rate and polymer concentration. Generally speaking, an increase in the amount of the polymer resulted in particles of enlarged diameters, while higher flow rates are advised if particles of reduced diameters are desired.

Although, the use of glycofurol as an excipient appeared to result in a more robust process with regards to physicochemical characteristics of the generated colloids, further characterization (AUC and TEM) revealed a large amount of small particles and non-desolvated polymer that was not detected by DLS. Electron microscopy also indicated that those particles were of non-spherical shape. Interactions between the carbonyl groups of Eudragit® and hydroxyl groups in the PEG-chain of glycofurol have been reported previously [29]. Therefore, it is likely that the strong interactions between these two excipients had an impact on the mode of precipitation due to an altered viscosity of the polymer solution and solubility of both polymers in combination.

The particle synthesis from ethanolic solution was rather sensitive to the investigated process parameters. As seen in Fig. 3a, slow flow rates resulted in particles of significantly increased diameter. This effect was even more pronounced when higher polymer concentrations were selected. Moreover, a broad size distribution as indicated by increased PDI values was observed. A PDI below 0.3 was accomplished when flow rates greater than 5.41 mL/min were adjusted (see Fig. 3c). Under these conditions, a rapid supersaturation of the polymer solution was achieved [23]. Therefore, a further

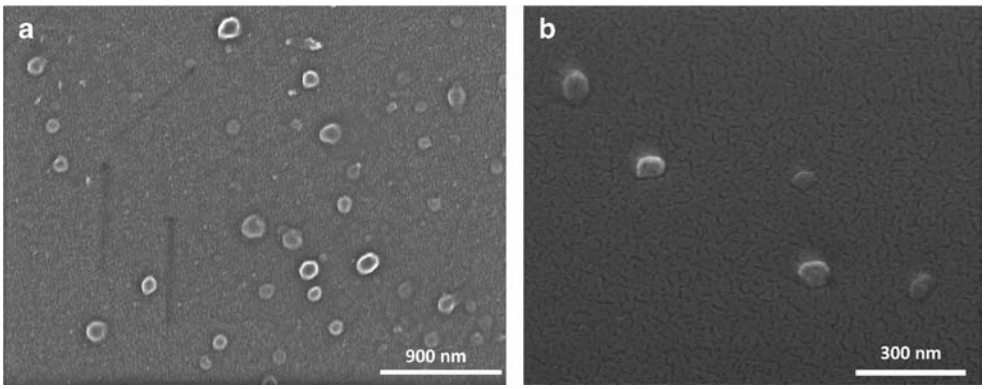

Fig. 11 SEM-images of nanoparticles gained by microreactor assisted nanoprecipitation at flow rates of 0.1 mL/min (polymer solution) to 0.3 mL/min (stabilizer solution) (**a**) or 0.5 to 1.5 mL/min (**b**), respectively.

increase in flow rate had only minor impact on product properties compared to the formulation design.

DLS is a relatively quick and efficient method for the determination of particle size, PDI, and zeta potential during early formulation development. However, since calculations of particle size and size distribution are based on scattering intensity fluctuations, the assumption is based upon a single light scattering signature by each particle [28]. Therefore, spherical particles are required for an accurate measurement.

Since only for nanoprecipitation from ethanolic solutions the particle size distribution observed by DLS could be confirmed by AUC, SEM, and TEM-results, DLS was validated as the primary analytical tool for these formulations. The alternative formulation design utilizing glycofurol evoked modified colloid properties in a way that particles outside the specification range occurred.

These results are in accordance to the precipitation efficiencies quantified for the two different formulation designs. While sedimentation of particles and the separation of particle fractions by centrifugation depend on the particle diameter, a higher amount of small particles in the glycofurolic suspensions decreased the measured precipitation efficiency dramatically.

The absolute value of the zeta potential indicated that the surface charge of the colloidal dosage form was constantly higher than +50 mV. Changes in formulation design remained irrelevant to this characteristic. Positively charged nanocarrier devices are efficiently internalized into cells [30]. The electrostatic interaction with the negatively charged cell plasma membrane is described as a key parameter for this cellular uptake by adsorptive endocytosis [31]. Moreover, the nanosized system exhibited high stability with regards to agglomeration and aggregation due to a strong electrostatic repulsion between the particles [32].

The optimal formulation design determined by the DoE was successfully applied to the preparation of photosensitizer loaded nanoparticles. For this purpose, the selected parameters were defined by an ethanolic Eudragit® RS 100 solution at a concentration of 15% [m/v] and a flow rate of 12 mL/min for the stabilizer, since thereby particles of optimal characteristics (particle size 193.1 ± 9.5 nm; PDI 0.167 ± 0.007) were yielded. Direct and indirect determination of drug loading efficiency in combination with the release characteristics confirmed a strong interaction between API and polymer. Although a considerable amount of the photosensitizer was not incorporated into the polymeric matrix, a sustained release compared to the pure API was observed in the release profile for formulations before and after purification. Consequently, the initial formulation design without further purification of the colloidal carrier was superior to the other formulation.

Since photodynamic activity is one important characteristic with regards to the efficacy of photosensitizers in photodynamic therapy (PDT) [7, 14], dark toxicity, and phototoxicity of mTHPC have been investigated *in vitro*. After illumination with light of a specific wavelength, the compound generates singlet oxygen and induces apoptosis and necrosis of the malignant cells [7, 14]. A number of drug delivery approaches utilize nanoparticles for the transport of photosensitizers into the tumor by taking advantage of passive and active drug targeting mechanism [7]. The observations in cell culture demonstrated superiority of the established formulation to the unprocessed API. While the efficacy that was measured in terms of the phototoxicity was not altered by the process step of encapsulation, the dark toxicity was significantly reduced. Hence, it is likely that side effects due to an increased light sensitivity are not to be expected. Furthermore, the purification process of the nanosized system did not exhibit advantages with regard to the efficacy and can therefore be neglected.

By translating the characteristics of the small scale preparation to medium scale manufacture, counterparts to the laboratory scale process parameters were identified for the microreactor-assisted nanoprecipitation. The advantages of those systems became obvious as they allow a facile adaption of experimental conditions within seconds, simple operation, and a high throughput [8, 9]. The approach bridged conventional batch production and continuous flow production by using a flow focusing microchannel system. The gas-liquid interaction induced a circulation in the channel that is

accompanied by a narrowed particle size distribution [9, 33]. Therefore, common limitation of microfluidic devices (e.g. insufficient size distribution, clogging of the nozzle, sticking to reactor walls) [8, 9] could be minimized with the established platform technology. An active control by the connected pumps assured rapid adaption of process parameters.

The factors SNS ratio and absolute flow rate could not be adopted without further modification, due to altered reaction conditions that are constituted by the dimension of the centerpiece and the impact of the nitrogen stream [9]. Nanoparticles with corresponding characteristics could be achieved when the ratio of polymer to aqueous solution was set to 1 part per 2 parts. Similar to the small scale experiments, higher polymer concentrations yielded particles of larger diameters also for this process. Therefore, no changes in polymer concentration were required. At an absolute flow rate of 2 mL/min and a polymer concentration of 15% [w/v], nanoparticles within the specification range (particle size 111.5± 6.3 nm) were achieved. Drug loading efficiency and the visual appearance confirmed the accomplishment of nanosized drug delivery systems with favorable characteristics.

The capacity of this system enabled a production of 4.5 g Eudragit® RS 100 nanoparticles per hour and is suitable for the supply of clinical studies. Moreover, an extremely robust process without significant clogging of the reaction chamber was observed for the investigated formulation design although the applied sustained release polymer typically adheres to metal surfaces. Therefore, progress over previously described continuous flow systems was achieved [8, 11]. Since the dimensions of the microreactor are predominantly important for the quality of the product, "scaling out" procedures can be used. Under such conditions an increased number of these microreactors multiply the output of the production process [34]. This strategy has been described for microfluidic droplet generators earlier [35]. At present, there are only few small companies that use such technologies for nanoencapsulation of pharmaceutical products [36].

The established continuous flow process depicts an ideal platform for integrated process analytical technology (PAT). The combination of Quality by Design principles and PAT is highly recommended by the Food and Drug Administration of the United States of America [37]. Product characteristics are accessible by real-time monitoring of particle size and particle size distribution e.g. by employing focused beam reflectance measurement® technology (Mettler-Toledo AutoChem Inc, Columbia, USA). Moreover, an on-line turbidity measurement could be conducted by shunting a flow-through cell. Consequently, nucleation rate and crystal growth could be monitored [38]. Changes in the concentration of API and excipient and the formation of new phases in the system could be monitored by near-infrared spectroscopy [37]. An option for the observation of size and shape of the yielded particle and detection of agglomerates would be the particle vision and measurement technology (Mettler-Toledo AutoChem Inc, Columbia, USA) [37, 38, 39]. These tools would complete the established preparation process and would replace the commonly used procedures of sampling and measurement performed by the pharmaceutical industry.

CONCLUSION

Bringing new nanomedicines to the market is still a challenge for manufacturers in the pharmaceutical industry. Since the regulatory framework requires a deeper understanding of formulation parameters relevant to their therapeutic efficacy and safety, only few technologies allow the production of nanocarriers under GMP-conditions [1].

The present investigation focused on the development of a well-defined formulation design and manufacturing process that allow distinct control of the most important product characteristics. By applying these technologies to the manufacture of Eudragit® RS 100 nanoparticles for PDT, a variety of physicochemical parameters such as particle size, size distribution, particle yield, and encapsulation efficiency have been adjusted. Most favorable characteristics were obtained for ethanolic Eudragit® RS 100 solutions at a concentration of 15% [w/v] that were precipiated with the 4-fold amount of a polysorbate 20 solution at a desolvation speed of 12 mL/min. For microreactor-assisted nanoprecipitation particles of similar characteristics were yielded at an absolute flow rate of 2 mL/min and a ratio of 1 part polymer solution to 2 parts stabilizer solution. Notable is the output of the established process. The enhanced process parameters allow the generation of 4.5 g polymeric nanoparticles per hour. Since the system was linked to a nitrogen stream, the increased pressure effectively prevented a clogging that is typically described as a problem for continuous flow processes. Therefore, a solid basis for a further transfer of the presented formulation to an industrial scale-production and upcoming stages of preclinical and clinical evaluation has successfully been achieved.

ACKNOWLEDGMENTS AND DISCLOSURES

The authors want to acknowledge Prof. Dr. Jennifer B. Dressman, Prof. Dr. Dieter Steinhilber, and Dr. Astrid Kahnt for their support and Evonik Industries AG for reagent supply.

This work has been supported by the Else Kröner-Fresenius Foundation (EKFS), Research Training Group Translational Research Innovation – Pharma (TRIP).

REFERENCES

1. Barenholz Y. Doxil® - the first FDA-approved nano-drug: lessons learned. J Control Release. 2012;160(2):117–34.

2. Lautenschlager C, Schmidt C, Lehr CM, Fischer D, Stallmach A. PEG-functionalized microparticles selectively target inflamed mucosa in inflammatory bowel disease. Eur J Pharm Biopharm. 2013;85(3 Pt A):578–86.
3. Lamprecht A, Schafer U, Lehr CM. Size-dependent bioadhesion of micro- and nanoparticulate carriers to the inflamed colonic mucosa. Pharm Res. 2001;18(6):788–93.
4. Lammers T, Kiessling F, Hennink WE, Storm G. Drug targeting to tumors: principles, pitfalls and (pre-) clinical progress. J Control Release. 2012;161(2):175–87.
5. Fessi H, Puisieux F, Devissaguet JP, Ammoury N, Benita S. Nanocapsule formation by interfacial polymer deposition following solvent displacement. Int J Pharm. 1989;55(1):1–4.
6. Langer K, Balthasar S, Vogel V, Dinauer N, von Briesen H, Schubert D. Optimization of the preparation process for human serum albumin (HSA) nanoparticles. Int J Pharm. 2003;257(1–2):169–80.
7. Oleinick NL, Evans HH. The photobiology of photodynamic therapy: cellular targets and mechanisms. Radiat Res. 1998;150(5 Suppl):146–56.
8. Karnik R, Gu F, Basto P, Cannizzaro C, Dean L, Kyei-Manu W, *et al.* Microfluidic platform for controlled synthesis of polymeric nanoparticles. Nano letters. 2008;8(9):2906–12.
9. Zhao C-X, He L, Qiao SZ, Middelberg AP. Nanoparticle synthesis in microreactors. Chemical Engineering Science. 2011;66(7):1463–79.
10. Santos RJ, Sultan MA. State of the art of mini/μ Jet reactors. Chemical Engineering & Technology. 2013;36(6):937–49.
11. Petschacher C, Eitzlmayr A, Besenhard M, Wagner J, Barthelmes J, Bernkop-Schnürch A, *et al.* Thinking continuously: a microreactor for the production and scale-up of biodegradable, self-assembled nanoparticles. Polymer Chemistry. 2013;4(7):2342–52.
12. Henderson BW, Dougherty TJ. How does photodynamic therapy work? Photochem Photobiol. 1992;55(1):145–57.
13. Bechet D, Couleaud P, Frochot C, Viriot ML, Guillemin F, Barberi-Heyob M. Nanoparticles as vehicles for delivery of photodynamic therapy agents. Trends Biotechnol. 2008;26(11):612–21.
14. Dougherty TJ. Photodynamic therapy (PDT) of malignant tumors. Crit Rev Oncol Hematol. 1984;2(2):83–116.
15. Bodmeier R, Chen H, Tyle P, Jarosz P. Spontaneous formation of drug-containing acrylic nanoparticles. J Microencapsul. 1991;8(2):161–70.
16. Viehof A, Javot L, Beduneau A, Pellequer Y, Lamprecht A. Oral insulin delivery in rats by nanoparticles prepared with non-toxic solvents. Int J Pharm. 2013;443(1–2):169–74.
17. Wacker M, Chen K, Preuss A, Possemeyer K, Roeder B, Langer K. Photosensitizer loaded HSA nanoparticles. I: Preparation and photophysical properties Int J Pharm. 2010;393(1–2):253–62.
18. Vogel V, Langer K, Balthasar S, Schuck P, Mächtle W, Haase W, et al. Characterization of serum albumin nanoparticles by sedimentation velocity analysis and electron microscopy. Analytical Ultracentrifugation VI: Springer; 2002. p. 31–36.
19. Bootz A, Vogel V, Schubert D, Kreuter J. Comparison of scanning electron microscopy, dynamic light scattering and analytical ultracentrifugation for the sizing of poly(butyl cyanoacrylate) nanoparticles. Eur J Pharm Biopharm. 2004;57(2):369–75.
20. Schuck P, Rossmanith P. Determination of the sedimentation coefficient distribution by least-squares boundary modeling. Biopolymers. 2000;54(5):328–41.
21. Porsch B, Hillang I, Karlsson A, Sundelof LO. Ion-exclusion controlled size-exclusion chromatography of methacrylic acid-methyl methacrylate copolymers. J Chromatogr A. 2000;872(1–2):91–9.
22. Dragicevic-Curic N, Scheglmann D, Albrecht V, Fahr A. Development of different temoporfin-loaded invasomes-novel nanocarriers of temoporfin: characterization, stability and in vitro skin penetration studies. Colloids Surf B Biointerfaces. 2009;70(2):198–206.
23. Wacker M, Zensi A, Kufleitner J, Ruff A, Schutz J, Stockburger T, *et al.* A toolbox for the upscaling of ethanolic human serum albumin (HSA) desolvation. Int J Pharm. 2011;414(1–2):225–32.
24. Wacker M. Nanocarriers for intravenous injection-the long hard road to the market. Int J Pharm. 2013;457(1):50–62.
25. Wacker MG. Nanotherapeutics-product development along the "nanomaterial" discussion. J Pharm Sci. 2014;103(3):777–84.
26. Moulari B, Pertuit D, Pellequer Y, Lamprecht A. The targeting of surface modified silica nanoparticles to inflamed tissue in experimental colitis. Biomaterials. 2008;29(34):4554–60.
27. Danhier F, Feron O, Preat V. To exploit the tumor microenvironment: Passive and active tumor targeting of nanocarriers for anticancer drug delivery. J Control Release. 2010;148(2):135–46.
28. Tscharnuter W. Photon correlation spectroscopy in particle sizing. In: Meyers RA, editor. Encyclopedia of analytical chemistry. Chinchester: Wiley; 2000. p. 5469–85.
29. Ali ME, Lamprecht A. Polyethylene glycol as an alternative polymer solvent for nanoparticle preparation. Int J Pharm. 2013;456(1):135–42.
30. Gratton SE, Ropp PA, Pohlhaus PD, Luft JC, Madden VJ, Napier ME, *et al.* The effect of particle design on cellular internalization pathways. Proc Natl Acad Sci U S A. 2008;105(33):11613–8.
31. Wang J, Byrne JD, Napier ME, DeSimone JM. More effective nanomedicines through particle design. Small. 2011;7(14):1919–31.
32. Muller RH, Jacobs C, Kayser O. Nanosuspensions as particulate drug formulations in therapy. Rationale for development and what we can expect for the future. Adv Drug Deliv Rev. 2001;47(1):3–19.33.
33. Günther A, Jhunjhunwala M, Thalmann M, Schmidt MA, Jensen KF. Micromixing of miscible liquids in segmented gas-liquid flow. Langmuir. 2005;21(4):1547–55.
34. Jensen KF. Microreaction engineering—is small better? Chemical Engineering Science. 2001;56(2):293–303.
35. Li W, Greener J, Voicu D, Kumacheva E. Multiple modular microfluidic (M 3) reactors for the synthesis of polymer particles. Lab on a Chip. 2009;9(18):2715–21.
36. Türeli AE, Penth B, Langguth P, Baumstümmler B. Vorrichtung und Verfahren zur Herstellung pharmazeutisch hochfeiner Partikel sowie zur Beschichtung solcher Partikel in Mikroreaktoren. German Patent Application DE102009008478A1; 2011.
37. Wu H, White M, Khan MA. Quality-by-Design (QbD): An integrated process analytical technology (PAT) approach for a dynamic pharmaceutical co-precipitation process characterization and process design space development. Int J Pharm. 2011;405(1–2):63–78.
38. Yu LX, Lionberger RA, Raw AS, D'Costa R, Wu H, Hussain AS. Applications of process analytical technology to crystallization processes. Adv Drug Deliv Rev. 2004;56(3):349–69.
39. Wu H, Khan MA. Quality-by-design: an integrated process analytical technology approach to determine the nucleation and growth mechanisms during a dynamic pharmaceutical coprecipitation process. J Pharm Sci. 2011;100(5):1969–86.